International Journal of GEOMATE, Oct. 2023, Vol. 25, Issue 110, pp.259-266
ISSN: 2186-2982 (P), 2186-2990 (O), Japan, DOI: https://doi.org/10.21660/2023.110.3984
Geotechnique, Construction Materials and Environment

SIZE-SCALE EFFECTS ON BENDING BEHAVIOUR OF NANOBEAM ON AN ELASTIC SUBSTRATE MEDIUM

Suchart Limkatanyu[1], *Worathep Sae-Long[2], Nattapong Damrongwiriyanupap[2], Apichat Buakla[2] and Preeda Chaimahawan[2]

[1]Department of Civil and Environmental Engineering, Faculty of Engineering, Prince of Songkla University, Thailand;
[2]Civil Engineering Program, School of Engineering, University of Phayao, Thailand

*Corresponding Author, Received: 17 June 2023, Revised: 16 Aug. 2023, Accepted: 23 Aug. 2023

ABSTRACT: This paper presents a new nonlocal beam-substrate medium model for the static bending analysis of micro- and nano-sized Euler-Bernoulli beam systems resting on an elastic substrate medium. The modified couple stress theory (MCST) represents the small-scale effect (nonlocal effect) inherent in micro- and nanoscale structures. The Winkler-Pasternak foundation model is used to model the characteristics of the underlying substrate medium, while the surface continuum model of Gurtin and Murdoch is employed to account for the size-dependent effect (surface-energy effect). The governing differential equation and its associated boundary conditions for the proposed beam-substrate medium model are derived based on the principle of virtual displacement. These equations are employed to assess the bending behavior of the nanobeam system on the elastic substrate medium. The analytical results are discussed through a numerical simulation, and this reveals that the small-scale effect, as well as size-dependent and substrate-structure interaction effects, lead to stiffness enhancement in the system.

Keywords: Modified couple stress theory, Small-scale effect, Size-dependent effect, Winkler-Pasternak foundation; Beam-substrate medium model

1. INTRODUCTION

In the recent year, nanotechnology has been developed, resulting in superior properties and higher-performance materials in engineering applications such as nanowire [1], biosensors [2], actuators [3], etc. For safety in design and use in these nano-applications, an in-depth study on both static and dynamic behaviors of these nanostructure systems is of great importance and is required. However, there are several limitations on the experimental tests of these nanosized structures, such as test equipment size, testing cost, and expertise in testing [4-5]. Therefore, rational structural models to predict both the static and dynamic behaviors of the nanostructures are required.

In the basic concept to develop the rational models, several higher-order elasticity theories have been employed to represent the small-scale effect (nonlocal effect) inherent in micro- and nanoscale structures, such as strain gradient theory [6], nonlocal elasticity theory [7], modified couple stress theory (MCST) [8], and modified strain gradient theory (MSGT) [4]. The MCST is one of these theories that has become popular in the last two decades to address the small-scale effect inherent in micro- and nanoscale structures. For example, Espo et al. [9] developed the piezoelectric phononic crystal nanobeam based on the MCST for the flexure wave band structure analysis, while Estabragh and Baradaran [10] developed the finite beam model based on the MCST to investigate the large deflection of the nanobeam. Jazi [11] employed the MCST to enhance the Timoshenko beam for the nonlinear force vibration analysis of an elastically connected double nanobeam system. Abouelregal and Marin [12] used the MCST to develop the Euler-Bernoulli beam model for the investigation of the temperature-dependent properties within the nanobeam. All those research works [9-12] confirmed the capability of the MCST to represent the small-scale effect in the nanostructures.

To represent the size-dependent effect due to the surface stress and its residual, Gurtin and Murdoch [13, 14] proposed the surface model. Due to its simplicity and capability, several works have used the Gurtin-Murdoch surface model to study the size-dependent effect inherent in micro- and nanoscale structures [15, 16].

According to the available nanobeam-substrate medium models, several works extend the MCST to develop the beam-substrate medium models [15, 17, 18]. For example, Limkatanyu et al. [15] enhanced the beam model on the Winkler foundation with the MCST to investigate the small-scale effect. Togun and Bağdatli [17] employed the MCST to develop the beam model on the Winkler foundation for the vibration analysis of the nanobeam on an elastic foundation, while Akbas [18] used a similar concept to study the force vibration analysis. However, to the best knowledge of the authors, there is no work that employed the MCST to develop the beam model on the Winkler-Pasternak foundation with the inclusion of the surface-energy effect for the bending analysis of the nanobeam on an elastic substate medium. Therefore, there is still room to develop and propose the rational beam-substrate medium model within the engineering fields.

This work employed the MCST [8], Gurtin-Murdoch surface model [13, 14], and Winkler-Pasternak foundation [19] to develop the beam-substrate medium model. The principle of virtual displacement is used to formulate the governing differential equation and its boundary conditions. Finally, a numerical simulation is employed to examine the small-scale, size-dependent, and substrate-structure interaction effects on the bending behavior of the nanobeam system on an elastic substrate medium.

2. KINEMATICS

Based on the Euler-Bernoulli beam theory [16], the deformed section of the nanobeam remains plane and normal to the longitudinal axis, as presented in Fig. 1. Therefore, the displacements at a particular point R, referred to by the reference axis, can be expressed as:

$$U_x(x,y) = -y\frac{dv_0(x)}{dx};\; U_y(x) = v_0(x);\; \text{and } U_z(x) = 0 \tag{1}$$

where $U_x(x,y)$, $U_y(x)$, and $U_z(x)$ are, respectively, the displacement fields along the x, y, and z axes; y is a distance measured from the reference axis; and $v_0(x)$ is the vertical displacement.

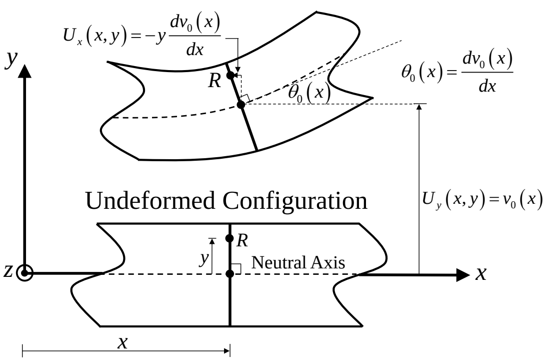

Fig.1 Kinematics of Euler-Bernoulli beam theory [16]

3. MODIFIED COUPLE STRESS THEORY

In order to represent the small-scale effect (nonlocal effect) on the classical beam model, this study applies the modified couple stress theory (MCST), as presented by Yang et al. [8] herein. The MCST is composed of the Cauchy stress and couple stress tensors, which are expressed as [15]:

$$\sigma_{ij} = \lambda\varepsilon_{kk}\delta_{ij} + 2\mu\varepsilon_{ij} \tag{2}$$

$$m_{ij} = 2l_m^2\mu\chi_{ij} \tag{3}$$

where σ_{ij} denotes the symmetric stress tensor, which is the conjugate-work pair of the strain tensor ε_{ij}; m_{ij} denotes the couple stress tensor, which is the conjugate-work pair of the symmetric curvature tensor χ_{ij}; λ and μ are the Lame constants; l_m denotes the material length-scale parameter; and δ_{ij} denotes the Kronecker delta.

The strain ε_{ij} and curvature tensor χ_{ij} are defined as [15]:

$$\varepsilon_{ij} = \frac{1}{2}\left(u_{i,j} + u_{j,i}\right) \tag{4}$$

$$\chi_{ij} = \frac{1}{2}\left(\theta_{i,j} + \theta_{j,i}\right) \tag{5}$$

where $u_{i,j}$ is the displacement gradient tensor; and $\theta_{i,j}$ is the rotation gradient tensor. The rotation vector θ_i can be written as [15]:

$$\theta_i = \frac{1}{2}e_{ijk}u_{k,j} \tag{6}$$

where e_{ijk} being the permutation symbol.

Based on the kinematics of the Euler-Bernoulli beam system of Eq. (1), the non-zero components of ε_{ij} and χ_{ij} can be written in terms of $v_0(x)$ as follows:

$$\varepsilon_{xx}(x,y) = -y\frac{d^2v_0(x)}{dx^2} \tag{7}$$

$$\chi_{xz}(x) = \chi_{zx}(x) = \frac{1}{2}\frac{d^2v_0(x)}{dx^2} \tag{8}$$

The non-zero components of σ_{ij} and m_{ij} in terms of $v_0(x)$ can be determined by substituting the $\varepsilon_{xx}(x,y)$ and $\chi_{xz}(x)$ of Eqs. (7) and (8) into the constitutive relations of Eqs. (2) and (3) as follows:

$$\sigma_{xx}(x,y) = -yE\frac{d^2v_0(x)}{dx^2} \tag{9}$$

$$m_{xz}(x) = m_{zx}(x) = l_m^2\mu\frac{d^2v_0(x)}{dx^2} \tag{10}$$

where E denotes the elastic modulus.

The Lame constants λ and μ can be written in terms of E and ν (Poisson's ratio) as [15]:

$$\lambda = \frac{E\nu}{(1+\nu)(1-2\nu)} \text{ and } \mu = \frac{E}{2(1+\nu)} \tag{11}$$

It is worthy to note that the Poisson's ratio is neglected in this study.

4. SURFACE ELASTICITY THEORY

According to the surface continuum models, Gurtin and Murdoch [13, 14] presented the surface model to reflect the size-dependent effect inherent in micro- and nano-sized structures based on surface continuum models. The bulk core and surface layer make up the beam's cross section. The beam core-surface layer bond is considered to be perfect, and the surface layer is regarded as a zero-thickness layer, as shown in Fig. 2. Under these hypotheses, the in-plane and out-of-plane surface stresses for the planer Euler-Bernoulli beam system are given by Limkatanyu et al. [16] as:

$$\tau_{xx}^{sur}(x,y) - \tau_0^{sur} = E^{sur}\varepsilon_{xx}^{sur}(x,y) \tag{12}$$

$$\tau_{nx}^{sur}(x) = \tau_0^{sur}\varepsilon_{nx}^{sur}(x) \tag{13}$$

where $\tau_{xx}^{sur}(x,y)$ denotes the in-plane surface stress, which is the conjugate-work pair of the surface strain $\varepsilon_{xx}^{sur}(x,y)$; $\tau_{nx}^{sur}(x)$ denotes the out-of-plane surface stress, which is the conjugate-work pair of the surface deformation $\varepsilon_{nx}^{sur}(x)$; τ_0^{sur} denotes the residual surface stress [16]; and $E^{sur} = \lambda^{sur} + 2\mu^{sur}$ denotes the surface elastic modulus obtained from the elastic constants λ^{sur} and μ^{sur}.

Based on the kinematics of Euler-Bernoulli beam of Eq. (1), the surface compatibility equations can be expressed as [16]:

$$\varepsilon_{xx}^{sur}(x,y) = \varepsilon_{xx}(x,y) = -y\frac{d^2v_0(x)}{dx^2} \tag{14}$$

$$\varepsilon_{nx}^{sur}(x) = n_y\frac{dv_0(x)}{dx} \tag{15}$$

where n_y is the unit vector on the y-component.

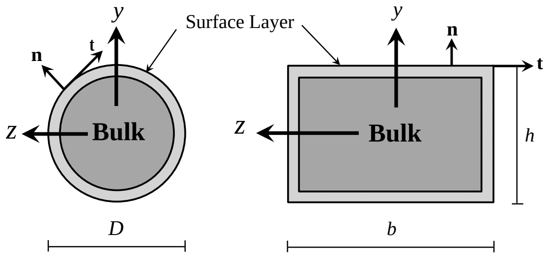

Fig.2 Gurtin and Murdoch surface model [13,14]

Substituting the surface compatibility of Eqs. (14) and (15) into the surface constitutive relations of Eqs. (12) and (13), we have:

$$\tau_{xx}^{sur}(x,y) - \tau_0^{sur} = -yE^{sur}\frac{d^2v_0(x)}{dx^2} \tag{16}$$

$$\tau_{nx}^{sur}(x) = n_y\tau_0^{sur}\frac{dv_0(x)}{dx} \tag{17}$$

5. WINKLER-PASTERNAK MODEL

This study uses the Winkler-Pasternak foundation model [19] to represent the nanobeam-substrate medium interaction. The underlying substrate medium is modeled as a non-interaction spring attached to the shear layer for this foundation model, as illustrated in Fig. 3. The constitutive relations of the Winkler-Pasternak model, as proposed by Limkatanyu et al. [19], are as follows:

$$D_{sub}(x) = k_{sub}v_{sub}(x) \tag{18}$$

$$V_{sub}(x) = G_{sub}\gamma_{sub}(x) \tag{19}$$

where k_{sub} and G_{sub} are the substrate medium stiffness and shear layer stiffness; $D_{sub}(x)$ and $V_{sub}(x)$ are the interactive force of the substrate medium and shear layer; and $v_{sub}(x)$ and $\gamma_{sub}(x)$ are the deformation of the substrate medium and shear layer, respectively.

The compatibility relations between the underlying substrate medium and nanobeam are given by Limkatanyu et al. [19] and assume that the bond between the nanobeam and substrate medium is perfect, resulting in the following relations:

$$v_{sub}(x) = v_0(x) \tag{20}$$

$$\gamma_{sub}(x) = \frac{dv_0(x)}{dx} \tag{21}$$

The foundation force-displacement relations are obtained by substituting the relations of Eqs. (20) and (21) into Eqs. (18) and (19), resulting in the following equations:

$$D_{sub}\left(x\right)=k_{sub}v_0\left(x\right) \tag{22}$$

$$V_{sub}\left(x\right)=G_{sub}\frac{dv_0\left(x\right)}{dx} \tag{23}$$

6. FORMULATION

6.1 Governing Differential Equation and Its Boundary Conditions: Displacement Approach

The notion of virtual displacement is used to obtain the governing differential equation and its boundary conditions for the proposed model. The overall virtual work can be written in the following general form:

$$\delta W=\delta W_{\text{int}}+\delta W_{\text{ext}} \tag{24}$$

where δW , δW_{int} , and δW_{ext} are, respectively, the total, internal, and external virtual work.

The internal and external virtual works of the proposed model can be expressed as:

$$\begin{aligned}\delta W_{\text{int}}=&\int_L\left(\int_A\sigma_{xx}\left(x,y\right)dA\right)\delta\varepsilon_{xx}\left(x,y\right)dx\\&+\int_L\left(\int_A 2m_{xz}\left(x\right)dA\right)\delta\chi_{xz}\left(x\right)dx\\&+\int_L\left(\oint_\Gamma\left(\tau_{xx}^{sur}\left(x,y\right)-\tau_0^{sur}\right)d\Gamma\right)\delta\varepsilon_{xx}^{sur}\left(x,y\right)dx\\&+\int_L\left(\oint_\Gamma\tau_{nx}^{sur}\left(x\right)d\Gamma\right)\delta\varepsilon_{nx}^{sur}\left(x\right)dx\\&+\int_L D_{sub}\left(x\right)\delta v_{sub}\left(x\right)dx\\&+\int_L V_{sub}\left(x\right)\delta\gamma_{sub}\left(x\right)dx\end{aligned} \tag{25}$$

$$\delta W_{\text{ext}}=-\int_L w_y\left(x\right)\delta v_0\left(x\right)dx-\delta\mathbf{U}^T\mathbf{P} \tag{26}$$

where A and Γ are, respectively, the sectional area and perimeter; $w_y\left(x\right)$ is the external transverse load; $\mathbf{P}=\left[P_1\quad P_2\quad P_3\quad P_4\right]^T$ is the force vector, which contains the end forces at boundaries; and $\mathbf{U}=\left[U_1\quad U_2\quad U_3\quad U_4\right]^T$ is the displacement vector, which contains the end displacements at boundaries.

Substituting the internal and external virtual works of Eqs. (25) and (26) and the compatibility relations of Eqs. (7), (8), (14), (15), (20), and (21) into Eq. (24), the total virtual work δW can be rewritten as:

$$\begin{aligned}\delta W=&\int_L M_{\sigma_{xx}}\left(x\right)\frac{d^2\delta v_0\left(x\right)}{dx^2}dx+\int_L M_{xz}\left(x\right)\frac{d^2\delta v_0\left(x\right)}{dx^2}dx\\&+\int_L M^{sur}\left(x\right)\frac{d^2\delta v_0\left(x\right)}{dx^2}dx+\int_L V^{sur}\left(x\right)\frac{d\delta v_0\left(x\right)}{dx}dx\\&+\int_L V_{sub}\left(x\right)\frac{d\delta v_0\left(x\right)}{dx}dx+\int_L D_{sub}\left(x\right)\delta v_0\left(x\right)dx\\&-\int_L w_y\left(x\right)\delta v_0\left(x\right)dx-\delta\mathbf{U}^T\mathbf{P}=0\end{aligned} \tag{27}$$

where $M_{\sigma_{xx}}\left(x\right)=-\int_A y\sigma_{xx}\left(x,y\right)dA$ denotes the sectional bending moment of the nanobeam; $M_{xz}\left(x\right)=\int_A m_{xz}\left(x\right)dA$ denotes the sectional bending moment caused by the couple stress; $M^{sur}\left(x\right)=-\oint_\Gamma y\left(\tau_{xx}^{sur}\left(x,y\right)-\tau_0^{sur}\right)d\Gamma$ denotes the sectional bending moment caused by the in-plane surface stress; and $V^{sur}\left(x\right)=\oint_\Gamma n_y\tau_{nx}^{sur}\left(x\right)d\Gamma$ denotes the sectional shear force caused by the out-of-plane surface stress.

To relocate the differential operators, the integration by part is applied, yielding the following equation:

$$\begin{aligned}\delta W=&\int_L\delta v_0\left(x\right)\left[\begin{array}{l}\dfrac{d^2M\left(x\right)}{dx^2}-\dfrac{dV_{eff}\left(x\right)}{dx}\\+D_{sub}\left(x\right)-w_y\left(x\right)\end{array}\right]dx\\&+\delta v_0\left(x\right)\left[\underbrace{-\frac{dM\left(x\right)}{dx}+V_{eff}\left(x\right)}_{V\left(x\right)}\right]_{x=0}^{x=L}\\&+\frac{d\delta v_0\left(x\right)}{dx}\left[M\left(x\right)\right]_{x=0}^{x=L}-\delta\mathbf{U}^T\mathbf{P}=0\end{aligned} \tag{28}$$

where $M\left(x\right)=M_{\sigma_{xx}}\left(x\right)+M_{xz}\left(x\right)+M^{sur}\left(x\right)$ denotes the total sectional bending moment; and $V_{eff}\left(x\right)=V^{sur}\left(x\right)+V_{sub}\left(x\right)$ denotes the effective sectional shear force.

Based on Eq. (28), the total sectional shear force $V\left(x\right)$ is:

$$V\left(x\right)=-\frac{dM\left(x\right)}{dx}+V_{eff}\left(x\right) \tag{29}$$

The relation of Eq. (28) can be rewritten based on the Cartesian sign convention as:

$$
\begin{aligned}
\delta W = \int_L \delta v_0(x) & \left[\begin{aligned} & \frac{d^2 M(x)}{dx^2} - \frac{dV_{eff}(x)}{dx} \\ & + D_{sub}(x) - w_y(x) \end{aligned} \right] dx \\
& - \delta U_1 \left[P_1 + \left(-\frac{dM(x)}{dx} + V_{eff}(x) \right) \right]_{x=0} \\
& - \delta U_2 \left[P_2 + \left(M(x) \right) \right]_{x=0} \\
& - \delta U_3 \left[P_3 - \left(-\frac{dM(x)}{dx} + V_{eff}(x) \right) \right]_{x=L} \\
& - \delta U_4 \left[P_4 - \left(M(x) \right) \right]_{x=L} = 0
\end{aligned}
\tag{30}
$$

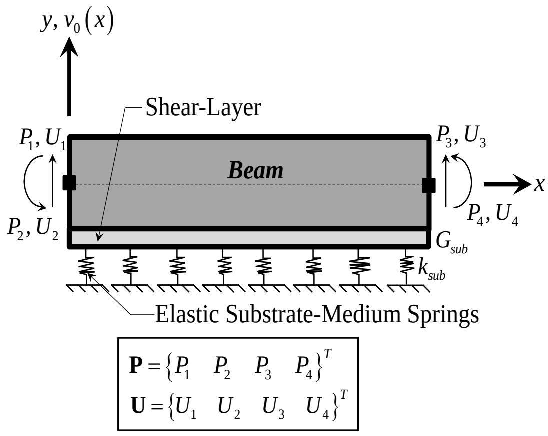

Fig.3 Concept of beam-substrate medium model [19]

By considering the arbitrariness of $\delta v_0(x)$, the governing differential equilibrium equation and its boundary conditions of the proposed model can be expressed as:

$$
\frac{d^2 M(x)}{dx^2} - \frac{dV_{eff}(x)}{dx} + D_{sub}(x) - w_y(x) = 0 \tag{31}
$$

$$
\begin{aligned}
& P_1 = -\left(-\frac{dM(x)}{dx} + V_{eff}(x) \right)_{x=0} ; \; P_2 = -\left(M(x) \right)_{x=0} ; \\
& P_3 = \left(-\frac{dM(x)}{dx} + V_{eff}(x) \right)_{x=L} ; \; P_4 = \left(M(x) \right)_{x=L}
\end{aligned}
\tag{32}
$$

By imposing the constitutive relation of Eqs. (9), (10), (16), (17), (22), and (23) into Eqs. (31) and (32), the governing differential equilibrium equation and its boundary conditions for the nanobeam system resting on the elastic substrate medium in Fig. 4 can be written in terms of $v_0(x)$ as:

$$
\begin{aligned}
& (EI)_{eff}^H \frac{d^4 v_0(x)}{dx^4} - (GA)_{eff}^H \frac{d^2 v_0(x)}{dx^2} \\
& + k_{sub} v_0(x) - w_y(x) = 0 \qquad \text{for } x \in [0, L]
\end{aligned}
\tag{33}
$$

$$
\begin{aligned}
& P_1 = -\left(-(EI)_{eff}^H \frac{d^3 v_0(x)}{dx^3} + (GA)_{eff}^H \frac{dv_0(x)}{dx} \right)_{x=0} ; \\
& P_2 = -\left((EI)_{eff}^H \frac{d^2 v_0(x)}{dx^2} \right)_{x=0} ; \\
& P_3 = \left(-(EI)_{eff}^H \frac{d^3 v_0(x)}{dx^3} + (GA)_{eff}^H \frac{dv_0(x)}{dx} \right)_{x=L} ; \\
& P_4 = \left((EI)_{eff}^H \frac{d^2 v_0(x)}{dx^2} \right)_{x=L}
\end{aligned}
\tag{34}
$$

where $(EI)_{eff}^H = EI + \mu l_m^2 A + E^{sur} I_\Gamma$ denotes the higher-order effective flexure rigidity; $(GA)_{eff}^H = \tau_0^{sur} S_\Gamma + G_{sub}$ denotes the higher-order effective shear rigidity; $A = \int_A dA$ denotes the section area; $I = \int_A y^2 dA$ denotes the second moment area; $I_\Gamma = \oint_\Gamma y^2 d\Gamma$ denotes the second moment perimeter; and $S_\Gamma = \oint_\Gamma n_y^2 d\Gamma$.

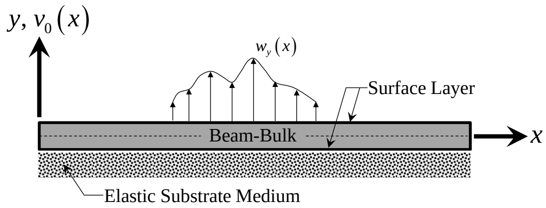

Fig.4 Nanobeam system resting on the elastic substrate medium subjected to the external load

6.2 Analytical Solutions

The general solutions of the governing differential equation of Eq. (33) are composed of the homogeneous solution $v_0^{HS}(x)$ and the particular solution $v_0^{PS}(x)$ as follows:

$$
v_0(x) = v_0^{HS}(x) + v_0^{PS}(x) \tag{35}
$$

The homogeneous solution $v_0^{HS}(x)$ is determined from Eq. (33) by neglecting the term of $w_y(x)$, while the particular solution $v_0^{PS}(x)$ considers this term ($w_y(x) \neq 0$). The general form of the homogeneous solutions $v_0^{HS}(x)$ in Eq. (35) stems from the solution of the beam model on the Winkler-Pasternak foundation, as proposed by Limkatanyu et al. [19] as:

$$v_0^{HS}(x) = C_1\psi_1(x) + C_2\psi_2(x) + C_3\psi_3(x) + C_4\psi_4(x) \quad (36)$$

where C_1, C_2, C_3, and C_4 are the constants from the integration; and $\psi_1(x)$, $\psi_2(x)$, $\psi_3(x)$, and $\psi_4(x)$ are the displacement functions, as presented in Appendix [19].

7. NUMERICAL SIMULATION

To investigate the size-scale effects on the bending behavior of the nanobeam on the substrate medium, a nanobeam system resting on the Winkler-Pasternak foundation subjected to a midspan concentrated load is employed herein and illustrated in Fig. 5. The geometric and material properties of the nanobeam are taken from Limkatanyu et al. [16] and are shown in Table 1, while the properties of the substrate medium are taken from Liew et al. [20] and Refaeinejad et al. [21]. The material length-scale parameter is defined to vary between 50 and 200 nm.

Table 1 Material properties of the nanobeam [16]

Material	Bulk modulus (MPa)	Poisson's ratio	Surface elastic modulus (nN/nm)	Residual surface stress (nN/nm)
Lead	16	0.4	8	0.63

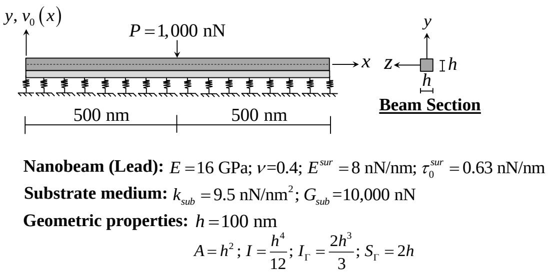

Fig.5 Simulation I: Bending analysis

Figure 6 depicts the vertical displacement pattern along the length of the nanobeam. When compared to the classical model (without the size-dependent and small-scale effects), the results show that both size-dependent and small-scale effects increase system stiffness, particularly the small-scale effect. The system stiffness increases as the material length-scale parameter l_m is increased.

To demonstrate the influence of the nanobeam-substrate medium interaction on bending behavior, the nanobeam-substrate medium system shown in Fig. 5 is used again, with the material length-scale parameter l_m set to 200 nm. The outcome is depicted in Fig. 7: Both the Winkler and Winkler-Pasternak models resulted in a stiffer system when compared to the model without foundation. As a result, it is possible to infer that the nanobeam-substrate medium interaction increases the stiffness of the system, particularly the Winkler-Pasternak foundation.

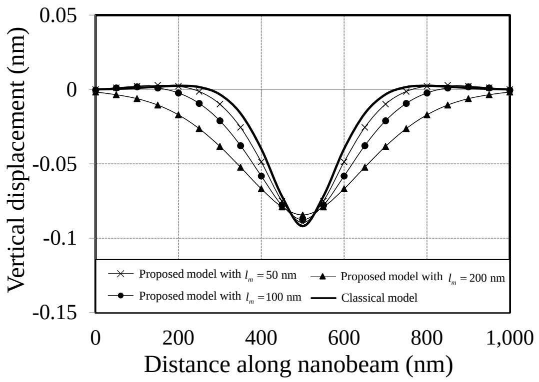

Fig.6 Influence of the small-scale and size-dependent effects on bending analysis

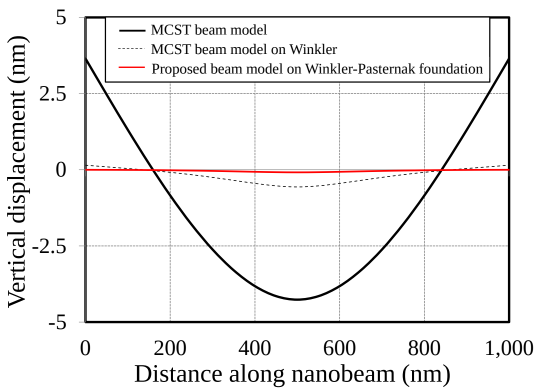

Fig.7 Influence of the nanobeam-substrate medium interaction effect on bending analysis

8. CONCLUSIONS

This paper proposes a novel beam-substrate model for the bending analysis of the nanobeam system on an elastic substrate medium. The small-scale and size-dependent effects are, respectively, represented through the modified couple stress theory and Gurtin-Murdoch surface model, while the nanobeam-substrate medium interaction effect is addressed based on the Winkler-Pasternak foundation. The associated differential equation and its boundary conditions of the proposed model are formulated based on the variational method and employed to assess and investigate the size-scale effects on the bending behavior. Finally, a numerical simulation is employed to examine the small-scale, size-dependent, and substrate-structure interaction effects on the bending behavior of the nanobeam system on an elastic substrate medium and can be concluded as follows:

- The small-scale, size-dependent, and nanobeam-substrate medium interaction effects lead to the stiffness enhancement of the nanobeam-substrate medium system.
- The system stiffness enhancement caused by the small-scale effect follows the increase in the material length-scale parameter l_m.
- Both Winkler and Winkler-Pasternak models show stiffer systems with nanobeam-substrate medium interaction, indicating increased stiffness, especially in the Winkler-Pasternak foundation.
- The small-scale, size-dependent, and nanobeam-substrate medium interaction effects are significant for the bending analysis of the nanostructures on the substrate medium.

9. ACKNOWLEDGMENTS

This study was financially supported by the Thailand Science Research and Innovation Fund and the University of Phayao (Grant No. FF66-UoE008) and the School of Engineering, University of Phayao, by the Thailand Research Fund (TRF) under Grant (RTA6280012), and by the National Research Council of Thailand (NRCT): Grant no. N25A650721.

10. REFERENCES

[1] Sae-Long W., Limkatanyu S., Sukontasukkul P., Damrongwiriyanupap N., Rungamornrat J., and Prachasaree W., Fourth-order strain gradient bar-substrate model with nonlocal and surface effects for the analysis of nanowires embedded in substrate media, Facta Univ. Ser. Mech. Eng., Vol.19, No.4, 2021, pp.657-680.

[2] Zare Y., Rhim S. S., and Rhee K. Y., The interphase degradation in a nanobiosensor including biopolymers and carbon nanotubes, Sens. Actuators, A, Vol. 331, 2021, 112967.

[3] Singh T. and Agrawal V. P., Concurrent design of a nanoactuator for “X-abilities” using the multiple-attribute decision-making approach, Concurrent Eng.: Res. Appl., Vol. 20, Issue 4, 2012, pp.301-314.

[4] Lam D. C. C., Yang F., Chong A. C. M., Wang J., and Tong P., Experiments and theory in strain gradient elasticity, J. Mech. Phys. Solids, Vol.51, Issue 8, 2003, pp.1477-1508.

[5] Gupta A. K., Nair P. R., Akin D., Ladisch M. R., Broyles S., Alam M. A., and Bashir R., Anomalous resonance in a nanomechanical biosensor, Appl. Phys. Sci., Vol.103, Issue 36, 2006, pp.13362-13367.

[6] Mindlin R. D., On the equations of elastic materials with micro-structure, Int. J. Solids. Struct., Vol.1, Issue 1, 1965, pp.73-78.

[7] Eringen A. C., Nonlocal polar elastic continua, Int. J. Eng. Sci., Vol. 10, Issue 1, 1972, pp.1-16.

[8] Yang F., Chong A. C. M., Lam D. C. C., and Tong P., Couple stress based strain gradient theory for elasticity, Int. J. Solids. Struct., Vol. 39, Issue 10, 2002, pp.2731-2743.

[9] Espo M., Hosseini S. M., and Abolbashari M. H., Bandgap characteristics of a piezoelectric phononic crystal Timoshenko nanobeam based on the modified couple stress and surface energy theories, Mater. Today Commun., Vol.33, 2022, 104782.

[10] Estabragh E. R. and Baradaran G. H., Analysis of large deflection of nanobeams based on the modified couple stress theory by using finite element method, Arch. Appl. Mech., Vol. 91, 2021, pp.4717-4734.

[11] Jazi S. H., Nonlinear vibration of an elastically connected double Timoshenko nanobeam system carrying a moving particle based on modified couple stress theory, Arch. Appl. Mech., Vol. 90, 2020, pp.2739-2754.

[12] Abouelregal A. E. and Marin M., The response of nanobeams with temperature-dependent properties using state-space method via modified couple stress theory, Symmetry, Vol.12, Issue 8, 2020, 1276.

[13] Gurtin M. E. and Murdoch A. I., A continuum theory of elastic material surface, Arch. Ration. Mech. Anal., Vol.57, 1975, pp.291-323.

[14] Gurtin M. E. and Murdoch A. I., Surface stress in solids, Int. J. Solids. Struct., Vol.14, Issue 6, 1978, pp.431-440.

[15] Limkatanyu S., Ponbunyanon P., Prachasaree W., Kuntiyawichai K., and Kwon M., Correlation between beam on Winkler-Pasternak foundation and beam on elastic substrate medium with inclusion of microstructure and surface effects, J. Mech. Sci. Technol., Vol.28, 2014, pp.3653-3665.

[16] Limkatanyu S., Sae-Long W., Rungamornrat J., Buachart C., Sukontasukkul P., Keawsawasvong S., and Chindaprasirt P., Bending, buckling and free vibration analyses of nanobeam-substrate medium systems, Facta Univ. Ser. Mech. Eng., Vol.20, No.3, 2022, pp.561-587.

[17] Togun N. and Bağdatli S., The vibration of nanobeam resting on elastic foundation using modified couple stress theory, Tehnički Glasnik, Vol.12, No.4, 2018, pp.221-225.

[18] Akbas S. D., Forced vibration analysis of

viscoelastic nanobeams embedded in an elastic medium, Smart Struct. Syst., Vol.18, Issue 6, 2016, pp.1125-1143.

[19] Limkatanyu S., Sae-Long W., Prachasaree W., and Kwon M., Improved nonlinear displacement-based beam element on a two-parameter foundation, Eur. J. Environ. Civ. Eng., Vol.19, Issue 6, 2015, pp.649-671.

[20] Liew K. M., He X. Q., and Kitipornchai S., Predicting nanovibration of multi-layered graphene sheets embedded in an elastic matrix, Acta Mater., V54, Issue 16, 2006, pp.4229-4236.

[21] Refaeinejad V., Rahmani O., Hosseini S. A., An analytical solution for bending, buckling, and free vibration of FG nanobeam lying on Winkler-Pasternak elastic foundation using different nonlocal higher order shear deformation beam theories, Sci. Iran., Vol.24, Issue 3, 2017, pp.1635-1653.

11. APPENDIX

The homogeneous solution $v_0^{HS}(x)$ of Eq. (36) depending on the values of the system parameters $\lambda_1 = k_{sub}/(EI)_{eff}^H$ and $\lambda_2 = (GA)_{eff}^H/(EI)_{eff}^H$ can be expressed as:

Case I: $\lambda_2 < 2\sqrt{\lambda_1}$

$$\begin{aligned} v_0^{HS}(x) = {} & C_1 \cosh[\alpha x]\cos[\beta x] \\ & + C_2 \sinh[\alpha x]\cos[\beta x] \\ & + C_3 \cosh[\alpha x]\sin[\beta x] \\ & + C_4 \sinh[\alpha x]\sin[\beta x] \end{aligned} \tag{A1}$$

Case II: $\lambda_2 > 2\sqrt{\lambda_1}$

$$\begin{aligned} v_0^{HS}(x) = {} & C_1 \cosh[\alpha x]\cosh[\beta x] \\ & + C_2 \sinh[\alpha x]\cosh[\beta x] \\ & + C_3 \cosh[\alpha x]\sinh[\beta x] \\ & + C_4 \sinh[\alpha x]\sinh[\beta x] \end{aligned} \tag{A2}$$

Case III: $\lambda_2 = 2\sqrt{\lambda_1}$

$$\begin{aligned} v_0^{HS}(x) = {} & C_1 e^{\sqrt[4]{\lambda_1}x} + C_2 x e^{\sqrt[4]{\lambda_1}x} \\ & + C_3 e^{-\sqrt[4]{\lambda_1}x} + C_4 x e^{-\sqrt[4]{\lambda_1}x} \end{aligned} \tag{A3}$$

where α and β are the auxiliary variables, which can be defined as:

$$\alpha = \sqrt{\frac{\sqrt{\lambda_1}}{2} + \frac{\lambda_2}{4}} \tag{A4}$$

$$\begin{aligned} & \beta = \sqrt{\frac{\sqrt{\lambda_1}}{2} - \frac{\lambda_2}{4}} \text{ for Case I; and} \\ & \beta = \sqrt{\frac{\lambda_2}{4} - \frac{\sqrt{\lambda_1}}{2}} \text{ for Case II} \end{aligned} \tag{A5}$$